Supporting Information

High entropy biphasic oxide cathode materials for sodium-ion batteries to mitigate performance degradation

Yusong Wang[a,b], Yingshuai Wang[a], Lei liu[a], Ziye Wang[a], Xiangyu Ding[a], Qinbo Zhou[a], Shaowen Huang[a,b], Hexiao Zhang[a], Hongcai Gao[a,b,c]*

a.School of Materials Science and Engineering, Beijing Institute of Technology, Beijing 100081, P.R. China
b.Yangtze Delta Region Academy of Beijing Institute of Technology, Jiaxing, 314019, China
c.Beijing Institute of Technology Chongqing Innovation Center, Chongqing 401120. P.R. China

Relevant formulas

The configuration entropy can be calculated from the following Eq. (S1)[1, 2]:

$$S_{config} = -R[(\sum_{i=1}^{N} x_i ln x_i)_{cation-site} + \sum_{j=1}^{M} x_j ln x_j)_{anion-site}] \quad \textbf{(S1)}$$

where R is the ideal gas constant (physics) and xi & xj are the mole fractions of the cationic and anionic site elements respectively. As the sample synthesised in the experiment contains only one anion, the influence of the anion has only a negligible effect on the Sconfig and the impact of the anion can not taken into consideration in the calculation. Moreover, the Gibbs free energy of the material can be calculated according to Eq. (S2)[1, 2]:

$$\Delta G = \Delta H - T\Delta S \quad \textbf{(S2)}$$

In the calculation of diffusion coefficients, if the relaxation time τ is very short, the relationship between $dE/d\sqrt{t}$ is linear, and the Na+ diffusion coefficient can be calculated by simplified Eq.(S3)[3]:

$$D_{Na+} = \frac{4}{\pi\tau}\left(\frac{m_B V_M}{M_B S}\right)^2\left[\frac{\Delta E_s}{\Delta E_t}\right]^2 \quad \textbf{(S3)}$$

where D_{Na+} (cm^2 s^{-1}) represents the Na+ diffusion coefficient, V_M (cm^3 mol^{-1}), m_B, and M_B are the molar volume, weight, and molar weight of the active materials, respectively, S and τ(s) denote the surface area of the electrode and the testing time in each step, and ΔE_s and ΔE_t are the quasi-equilibrium potential and the change in cell voltage *E* during the current pulse, respectively.

Figure

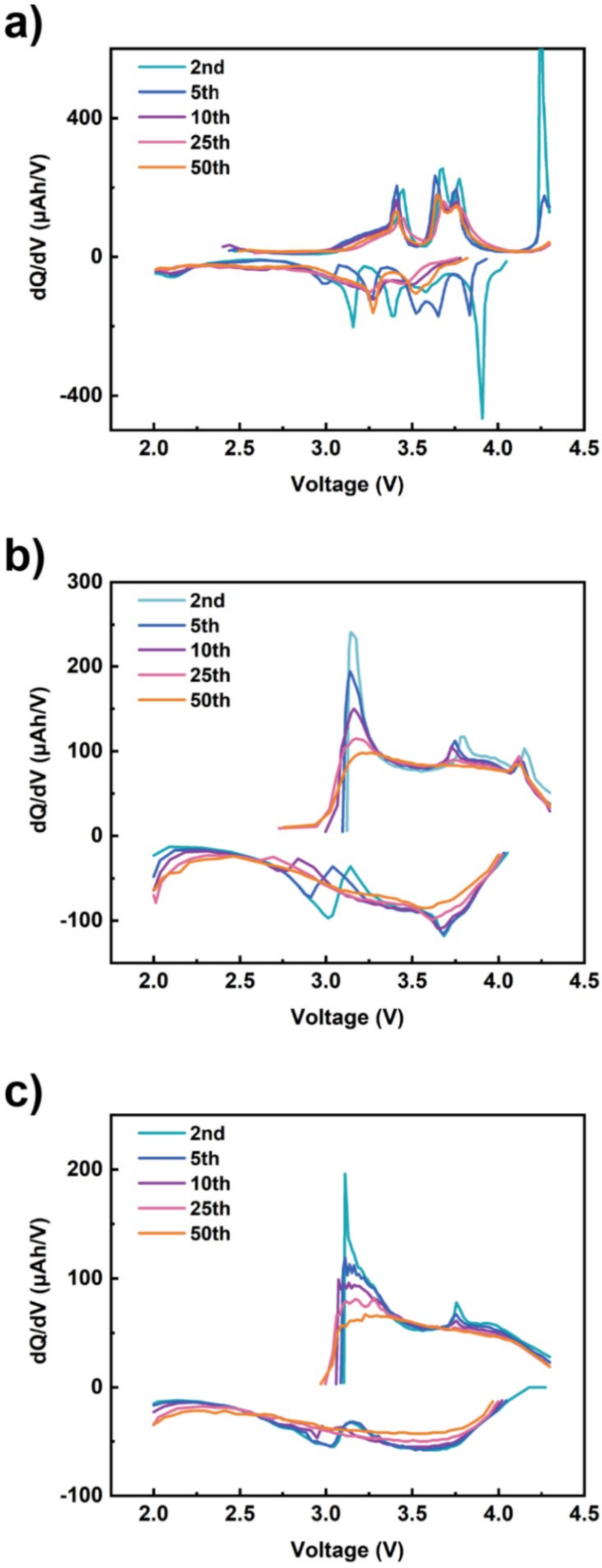

Fig. S1 dQ/dV curves for NNMO, O3-HEO and P2/O3-HEO.

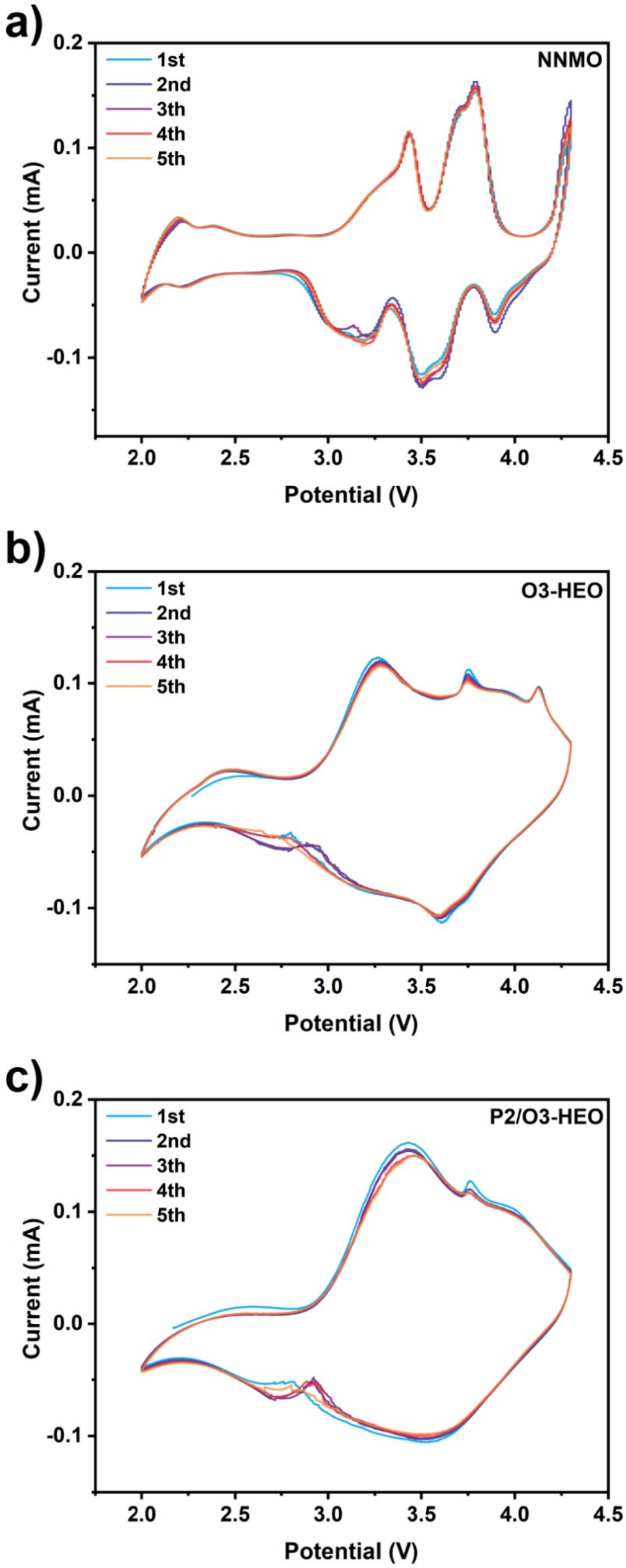

Fig. S2 CV curves of NNMO, O3-HEO and P2/O3-HEO at 0.3 mV s^{-1}

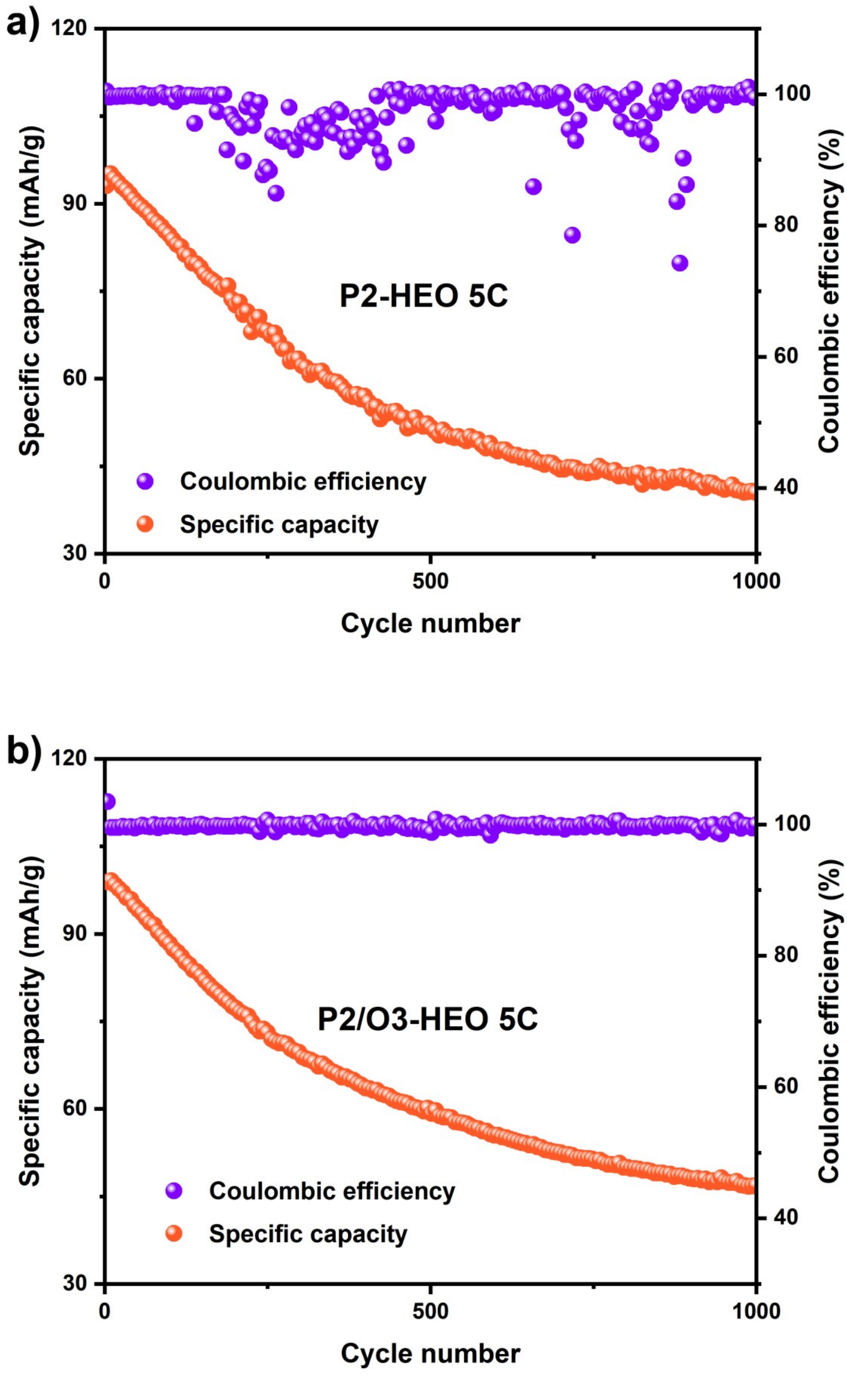

Fig. S3 The cycling performances at 5C for O3-HEO and P2/O3-HEO.

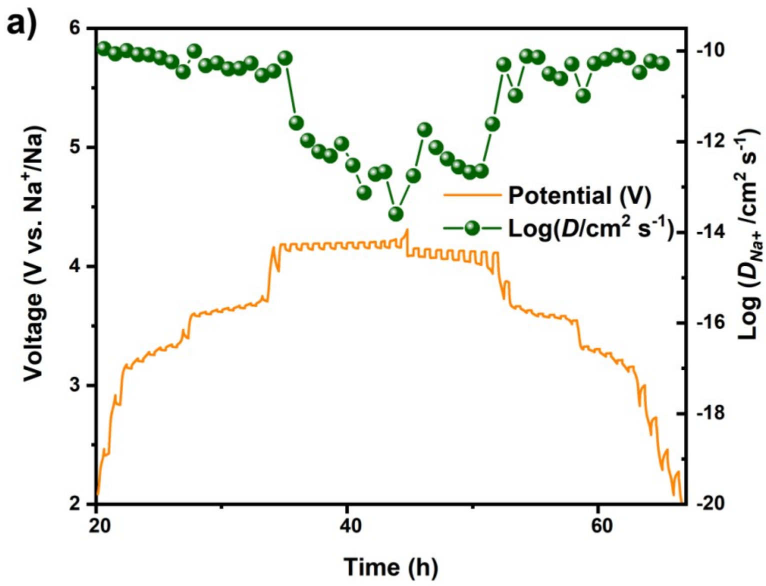

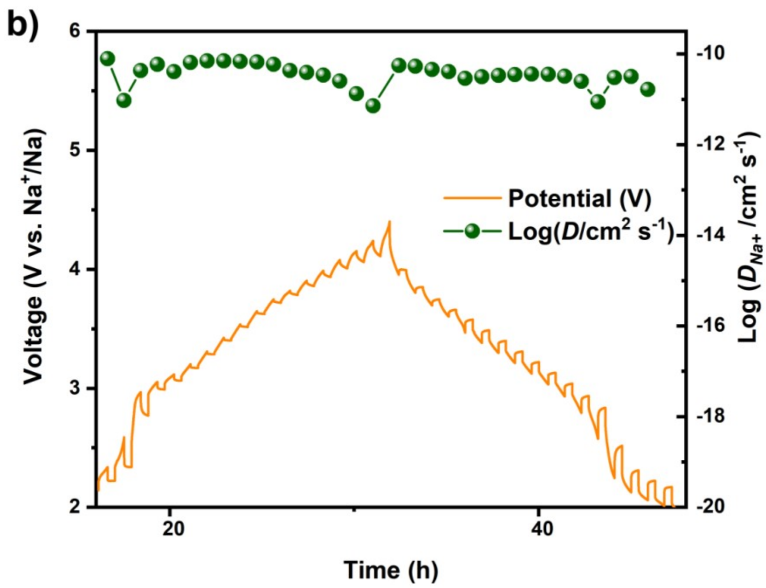

Fig. S4 GITT curves and corresponding D_{Na+} values of NNMO and O3-HEO.

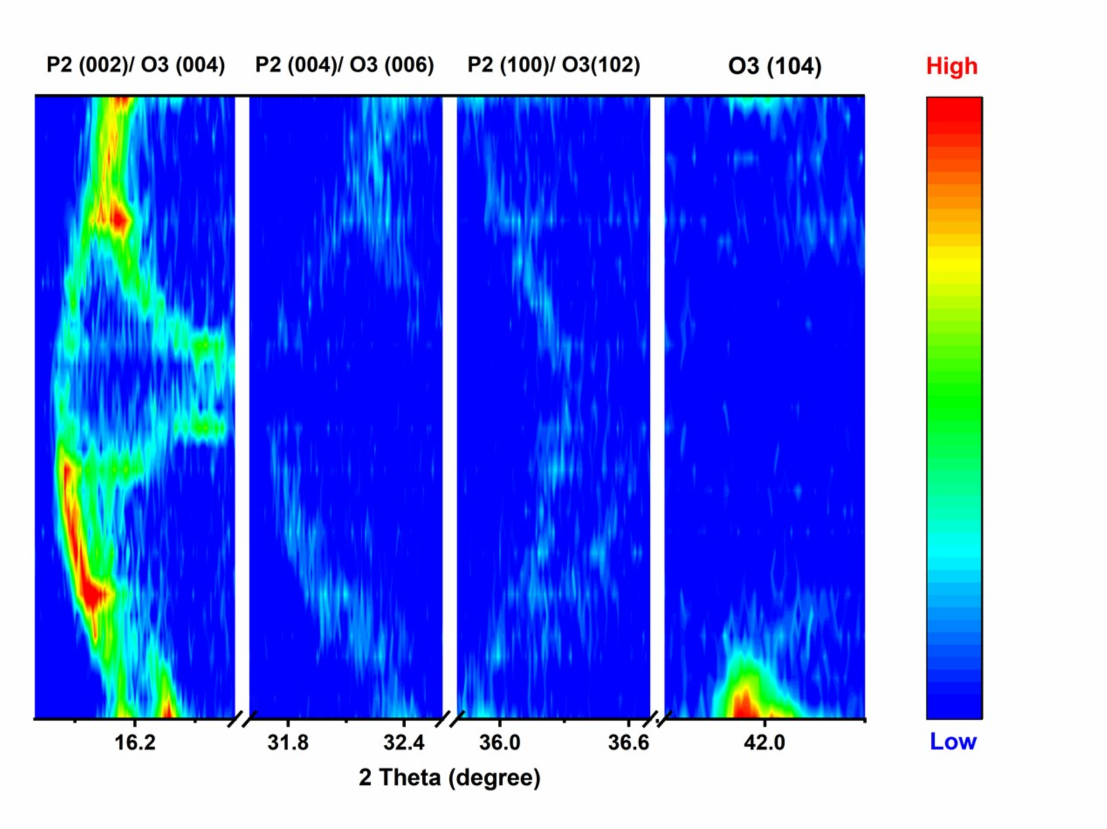

Fig. S5 The contour plot of In-situ XRD patterns selected 2θ regions.

Table

Table S1 Rietveld refinement result of P2/O3-HEO .

71.8 wt% O3 phase $R\bar{3}m$						
Atom	**Wyckoff**	**x**	**y**	**z**	**Occ.**	U_{iso}
Na	3a	0	0	0	0.802	0.0186
TM	3b	0	0	0.5	1	0.0250
O	6c	0	0	0.234	0.951	0.0017
a=b=2.94009 Å, c=16.44799 Å, V=123.130 Å^3, α=β=90°, γ=120°						
28.2 wt% P2 phase P63/mmc						
Atom	**Wyckoff**	**x**	**y**	**z**	**Occ.**	U_{iso}
Na_e	2d	0.66667	0.33333	0.25	0.392	0.2732
Na_f	2b	0	0	0.25	0.287	0.1010
TM	2a	0	0	0	1	0.0250
O	4f	0.66667	0.33333	0.08593	0.924	0.0250
a=b=2.91147 Å, c=11.13127 Å, V=81.715 Å^3, α=β=90°, γ=120°						
R_{wp} **= 5.411%, GOF = 3.23,** χ^2 **= 10.42**						

Table S2 Rietveld refinement result of O3-HEO .

O3 phase $R\bar{3}m$						
Atom	**Wyckoff**	**x**	**y**	**z**	**Occ.**	B_{iso}
Na	3a	0	0	0	0.919	0.0594
TM	3b	0	0	0.5	1	0.0250
O	6c	0	0	0.23250	0.947	0.0065
a=b=2.95741 Å, c=16.18838 Å, V=122.619 Å^3, α=β=90°, γ=120°						
Rwp = 5.462%, GOF = 2.52, χ2 = 6.34						

Table S3 Rietveld refinement result of NNMO .

P2 phase P63/mmc						
Atom	**Wyckoff**	**x**	**y**	**z**	**Occ.**	B_{iso}
Na_e	2d	0.66667	0.33333	0.25	0.389	0.2124
Na_f	2b	0	0	0.25	0.268	0.1067
TM	2a	0	0	0	1	0.0250
O	4f	0.66667	0.33333	0.08363	0.964	0.0065
a=b=2.88295 Å, c=11.1605 Å, V=80.332 Å^3, α=β=90°, γ=120°						
Rwp = 5.958%, GOF = 2.11, χ2 = 4.47						

Table S4 The XRF result of O3-HEO

	Na	Mn	Fe	Ti	Ni	Mg	Zn	Cu
mass fraction %	14.65	24.19	9.27	2.42	9.96	1.42	3.89	4.16
Composition of atomic	0.637	0.439	0.165	0.050	0.169	0.059	0.060	0.065

Table S5 The XRF result of P2/O3-HEO

	Na	Mn	Fe	Ti	Ni	Mg	Zn	Cu
mass fraction %	18.99	24.37	9.41	2.40	10.02	1.29	4.02	4.03
Composition of atomic	0.826	0.443	0.168	0.050	0.170	0.053	0.062	0.063

Table S6 Electrochemical performance comparison between this work and previously reported result

Cathode materials	**phase type**	**specific capacity (mAh g^{-1})**	**voltage window**	**cycle performance**	**refs**
$Na_{0.67}Fe_{0.425}Mn_{0.425}Mg_{0.15}O_2$	P2/O3	146.6 (0.1C)	1.5-4.2V	95.7%/1C, 50 cycles	[4]
$Na_{0.67}Fe_{0.5}Mn_{0.46}Mg_{0.04}O_2$	P2/O3	143.7 (1C)	1.5-4.2V	63.9%/1C, 70 cycles	[5]
$Na_{0.8}Ni_{0.4}Mn_{0.4}Ti_{0.2}O_2$	P2/O3	158 (0.1C)	2.0-4.2V	94%/0.5C, 200 cycles	[6]
$Na_{0.85}Ni_{0.34}Mn_{0.33}Ti_{0.33}O_2$	P2/O3	126.6 (0.1C)	2.2-4.4V	80.6%/1C, 200 cycles	[7]
$Na_{0.8}Mn_{0.6}Ni_{0.3}Cu_{0.1}O_2$	P2/O3	139 (0.1C)	1.5-4.2V	85%/0.2C, 100 cycles	[8]
$Na_{0.67}Fe_{0.425}Mn_{0.425}Cu_{0.15}O_2$	P2/O3	140.5 (0.1C)	2.0-4.2V	87.1%/1C, 100 cycles	[9]
$Na_{0.80}[Li_{0.12}Ni_{0.22}Mn_{0.66}]O_2$	P2	133 (0.1C)	2.0-4.4V	91%/0.1C, 50 cycles	[10]
$Na_{0.62}Mn_{0.67}Ni_{0.23}Cu_{0.05}Mg_{0.07}Ti_{0.01}O_2$	P2	148.2 (0.1C)	2.0-4.3V	87%/1C, 500 cycles	[2]
$NaLi_{0.1}Ni_{0.35}Mn_{0.55}O_2$	O3	160 (0.1C)	1.5-4.3V	85%/0.1C, 100 cycles	[11]
$NaNi_{0.32}Fe_{0.32}Mn_{0.32}Al_{0.02}Cu_{0.02}O_2$	O3	146 (0.1C)	2.0-4.0V	81%/1C, 200 cycles	[12]
P2/O3-HEO	P2/O3	162 (0.1C)	2.0-4.3V	72.9%/5C, 300 cycles	This work

Reference

1. A. Sarkar, Q. Wang, A. Schiele, M. R. Chellali, S. S. Bhattacharya, D. Wang, T. Brezesinski, H. Hahn, L. Velasco and B. Breitung, *Advanced Materials*, 2019, **31**, 1806236.
2. F. Fu, X. Liu, X. Fu, H. Chen, L. Huang, J. Fan, J. Le, Q. Wang, W. Yang, Y. Ren, K. Amine, S.-G. Sun and G.-L. Xu, *Nature Communications*, 2022, **13**, 2826.
3. Y. Fan, X. Ye, X. Yang, L. Guan, C. Chen, H. Wang and X. Ding, *Journal of Materials Chemistry A*, 2023, **11**, 3608-3615.
4. D. Zhou, W. Huang, X. Lv and F. Zhao, *Journal of Power Sources*, 2019, **421**, 147-155.
5. D. Zhou, C. Zeng, D. Ling, T. Wang, Z. Gao, J. Li, L. Tian, Y. Wang and W. Huang, *Journal of Alloys and Compounds*, 2023, **931**, 167567.
6. X. Ma, H. Guo, J. Gao, X. Hu, Z. Li, K. Sun and D. Chen, *Journal*, 2023, **13**.
7. L. Yu, Z. Cheng, K. Xu, Y.-X. Chang, Y.-H. Feng, D. Si, M. Liu, P.-F. Wang and S. Xu, *Energy Storage Materials*, 2022, **50**, 730-739.
8. S. Saxena, H. N. Vasavan, M. Badole, A. K. Das, S. Deswal, P. Kumar and S. Kumar, *Journal of Energy Storage*, 2023, **64**, 107242.
9. P. Zhang, G. Zhang, Y. Liu, Y. Fan, X. Shi, Y. Dai, S. Gong, J. Hou, J. Ma, Y. Huang and R. Zhang, *Journal of Colloid and Interface Science*, 2024, **654**, 1405-1416.
10. J. Xu, D. H. Lee, R. J. Clément, X. Yu, M. Leskes, A. J. Pell, G. Pintacuda, X.-Q. Yang, C. P. Grey and Y. S. Meng, *Chemistry of Materials*, 2014, **26**, 1260-1269.
11. S. Zheng, G. Zhong, M. J. McDonald, Z. Gong, R. Liu, W. Wen, C. Yang and Y. Yang, *Journal of Materials Chemistry A*, 2016, **4**, 9054-9062.
12. S. Feng, C. Zheng, Z. Song, X. Wu, M. Wu, F. Xu and Z. Wen, *Chemical Engineering Journal*, 2023, **475**, 146090.